# A Nearly Decentralized Voltage Regulation Algorithm for Loss Minimization in Radial MV Networks With High DG Penetration

Georgios C. Kryonidis, *Student Member, IEEE*, Charis S. Demoulias, *Senior Member, IEEE*, and Grigoris K. Papagiannis, *Senior Member, IEEE*

***Abstract*—In this paper, a nearly decentralized voltage regulation algorithm is proposed that effectively coordinates the operation of distributed generation (DG) units in order to minimize the active power losses and the total reactive power consumption in medium-voltage (MV) networks with radial topology. This control requires minimum communication infrastructure, whereas decisions are individually taken by each DG unit based on local and remote measurements. Furthermore, a new cooperative on-load tap changer control is employed to further reduce the network losses. The proposed controls are validated by time-domain and time-series quasi-static simulations in a radial MV network. The former highlights the fast response and the robustness of the proposed voltage regulation algorithm, while comparisons with well-known decentralized control schemes and an optimal power flow method show the improved performance of the proposed controls.**

***Index Terms*—Distributed generation, loss minimization, on-load tap changer, reactive power control, voltage regulation.**

## I. Introduction

NOWADAYS, the distribution grid is facing a transition towards the proliferation of distributed generation (DG), mainly due to the advent of renewable energy resources. This transition is promoted by local and international policies to improve flexibility, sustainability and efficiency [1]. This poses, however, new technical challenges concerning the smooth operation of the network such as: Protection problems, voltage regulation issues, and overloading of network equipment [2]. Among them, voltage rise is the most common issue prohibiting the further increase of DG penetration in medium- (MV) and low-voltage (LV) networks [3].

Considering MV networks, several solutions have been proposed to tackle the voltage rise problem. Grid reinforcement is an effective but expensive solution for the distribution system operators (DSOs). In [4], a coordinated operation of the on-load tap changer (OLTC) with step voltage regulators (SVRs) has been proposed to control the voltage profile. The main drawbacks of this method are the high infrastructure investments by means of installing new SVRs, while DG does not contribute in the voltage regulation process. However, the network performance can be significantly improved by the active participation of DG which is attained by applying reactive power control techniques [5]-[21].

In the literature, the reactive power-based control approaches are classified into three main categories: 1) centralized control, 2) distributed control, and 3) decentralized control. In the centralized control, reactive power control is centrally managed and an extended telecommunication infrastructure is required to efficiently monitor the distribution grid. In [5]-[7], multi-agent-based voltage control methods are proposed, employing the sensitivity matrix to dispatch the reactive power to DG units. Another form of centralized control is the optimal dispatch of DG units and network assets to satisfy an objective, e.g. minimizing the reactive power consumption or the network losses, resulting in a mixed-integer non-linear optimization problem [8]-[10]. Nevertheless, these approaches are time-consuming and may lead to suboptimal results.

In order to overcome the problems introduced by the centralized control, a distributed control approach for voltage regulation is proposed in [11] and [12]. Its distinct features are the lack of a central controller and the distributed way of communication among DG units. However, the convergence rate of this control is very slow and the optimal solution is not ensured.

In the decentralized approach, control actions are determined based only on local measurements, introducing robustness and flexibility in the network operation, whereas communication is only required for coordination purposes. In [13], each DG unit absorbs reactive power to compensate the voltage rise caused by the active power injection. The authors in [14] and [15] proposed a decentralized control which simultaneously regulates the voltage and minimizes network losses. However conflicts between these objectives may occur, especially under high penetration conditions. An updated version of [14] has been proposed in [16], where a central controller is used to choose the most appropriate objective function, based on the current network conditions.

The off-line coordination of the decentralized control

Manuscript received October 06, 2015; revised January 19, 2016, and March 7, 2016; accepted April 14, 2016.

The authors are with the School of Electrical and Computer Engineering, Aristotle University of Thessaloniki, Thessaloniki GR 54124, Greece (e-mail: grigoris@eng.auth.gr).



Citation Information: DOI: 10.1109/TSTE.2016.2556009

schemes has been introduced in [17]-[21]. More specifically, a coordinated calculation of $Q(P)$ and $Q(V)$ characteristics by employing the sensitivity matrix is proposed in [17] and [18], respectively. In [19]-[21], artificial intelligence techniques are applied to coordinate the decentralized operation of DG units. Nevertheless, these methods do not ensure the minimization of reactive power consumption or of the network losses during network operation.

In this paper, a nearly decentralized voltage regulation method is proposed that mainly aims at the minimization of active power losses in MV networks with radial topology. This is achieved by applying reactive power control to specific DG units and taking into account the network topology. The proposed method is based on minimum communication requirements, whereas the overall reactive power consumption is reduced and the maximum DG penetration is further increased, compared to other decentralized methods. Additionally, the combined operation of the proposed reactive power control with an improved OLTC operation is investigated to further reduce the network losses.

Following this introduction, Section II describes the problem formulation, while the proposed reactive power control method is analyzed in Section III. The updated OLTC operation is described in Section IV. Simulation results for a radial MV network are presented in Section V, where comparisons are made with existing methods to highlight the efficiency of the proposed control. Finally, discussion and conclusions are presented in Section VI.

## II. Problem Formulation

At the MV level, power distribution networks with radial topology are mainly located in rural areas with low population density. Most of the DG units deployed in these networks have an intermittent generation profile, e.g. PVs. This prompts DSOs to connect them in dedicated, generation-only feeders to mitigate the effect these DG units have on the conventional loads. A typical configuration of such a network is depicted in Fig. 1 comprising three feeder categories, namely mixed generation-consumption, only consumption and only generation.

In this network, voltage regulation can be attained either by allocating the reactive power among the DG units or by adjusting the tap position of the high-voltage/medium-voltage (HV/MV) transformer. In such a case, operational constraints, regarding the thermal limit of lines and the reactive power capability of DG units, must be also considered. Since the objective of the proposed control scheme is the minimization of the network active power losses, the problem can be formulated as a mixed-integer non-linear optimization problem, expressed mathematically as follows:

$$\min \sum_{i \in N} P_{loss,i}$$

s.t.

$$\begin{aligned} V_i^2 &= \left\{ \left[ V_{prev,i}^4 + 4\left(A_i R_i + B_i X_i\right) V_{prev,i}^2 - 4\left(A_i X_i - B_i R_i\right)^2 \right]^{1/2} \right. \\ &\quad \left. + V_{prev,i}^2 + 2\left(A_i R_i + B_i X_i\right) \right\} / 2 \quad \forall i \in N \\ P_{loss,i} &= R_i \left(A_i^2 + B_i^2\right) / V_i^2 \quad \forall i \in N \\ Q_{loss,i} &= X_i \left(A_i^2 + B_i^2\right) / V_i^2 \quad \forall i \in N \\ Q_{\min} &\le Q_i \le Q_{\max} \quad \forall i \in N_{DG} \\ V_{\min} &\le V_i \le V_{\max} \quad \forall i \in N \\ I_i &\le I_{\max} \quad \forall i \in N \\ Tap &\in D \end{aligned} \tag{1}$$

In the above equations which are derived from the power flow theory, $N$ denotes the set of network nodes and also of branches, $N_{DG}$ is the set of nodes with DG units, and $D$ is the discrete set of the transformer tap setting. $P_{loss,i}$ and $Q_{loss,i}$ is the active and reactive power loss of the $i$-th branch calculated with respect to the corresponding resistance ($R_i$) and reactance ($X_i$). $V_i$ and $V_{prev,i}$ is the voltage magnitude of the $i$-th node and of the previous adjacent node, respectively. $I_i$ is the current flowing through the $i$-th branch, whereas $Q_i$ is the reactive power produced by the DG unit located at the $i$-th node and $Tap$ is the tap position of the OLTC. Coefficients $A_i$ and $B_i$ are calculated according to:

$$A_i = \sum_{j \in N_{d,i}} P_j - \sum_{j \in N_{d,i+1}} P_{loss,j} \tag{2}$$

$$B_i = \sum_{j \in N_{d,i}} Q_j - \sum_{j \in N_{d,i+1}} Q_{loss,j} \tag{3}$$

$P_j$ and $Q_j$ denote the active and reactive power injections at the $j$-th node, whereas $N_{d,i}$ is the set of nodes located downstream of the $i$-th node.

Scope of this paper is to solve the above optimization problem in a decentralized and more robust manner, while keeping the minimum communication requirements. For this purpose, the OLTC and the reactive power control of the DG units are designed to act independently, but in a coordinated way, based on local and remote measurements. The voltage regulation with minimum losses is performed by the proposed reactive power control taking into account the network configuration, whereas the introduction of an updated version of the OLTC contributes to the further reduction of network losses.

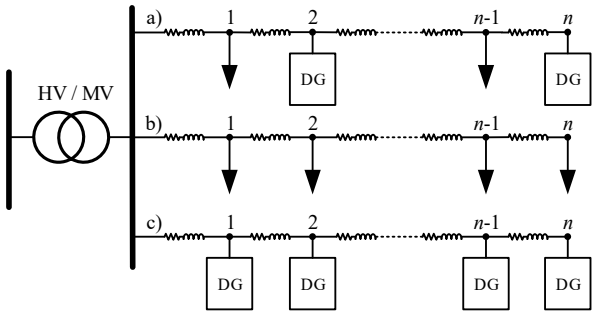


Fig. 1. MV network configuration consisting of three feeder types. (a) Mixed generation-consumption. (b) Only consumption. (c) Only generation.

## III. Proposed Reactive Power Control

The reactive power control is applied to feeders with installed DG units where voltage regulation issues, especially overvoltages, may arise. This often occurs at the generation feeder depicted in Fig. 2 due to the reverse power flow caused by the injection of DG units. On the other hand, overvoltages are less likely to happen in the mixed generation-consumption feeder, since the DG penetration is restricted by many DSOs to cause only 3 % voltage rise with respect to the case with no generation [22]. This limitation aims to mitigate the technical issues that arise by the DG connection in this feeder, such as increased short circuit level at the point of common coupling (PCC), current congestion, continuous voltage deviations etc. [2]. Therefore, the proposed reactive power control needs to be examined for the generation-only feeder. In the next subsections, the theoretical framework and the actual implementation of this control are presented.

### A. Theoretical Framework

The reactive power allocation for loss minimization is a non-linear optimization problem as shown in (1). A decentralized solution to this problem is given by employing the sensitivity theory which linearizes the network. Therefore, analytical expressions, which describe the relation among the reactive power of the DG units, the corresponding voltages and the network losses, can be derived leading to the proposed reactive power control. More specifically, the sensitivity theory is employed to the generation feeder depicted in Fig. 2, which consists of unevenly distributed DG units. Thus, the voltage magnitude ($\Delta V$) and angle ($\Delta\theta$) variations are quantified with respect to active and reactive power injections according to:

$$\begin{bmatrix}\Delta\theta\\ \Delta V\end{bmatrix} = S\begin{bmatrix}\Delta P\\ \Delta Q\end{bmatrix} = \begin{bmatrix}S_P^{\theta} & S_Q^{\theta}\\ S_P^{V} & S_Q^{V}\end{bmatrix}\begin{bmatrix}\Delta P\\ \Delta Q\end{bmatrix} \tag{4}$$

In (4) $S$ is the sensitivity matrix, consisting of four submatrices corresponding to the partial derivatives of node voltage magnitude and angle against active and reactive power. Due to the incorporation of reactive power control schemes in DG units as a voltage regulation means, the sensitivity of voltage magnitude to reactive power variations is of main interest and can be approximated, as proposed in [23], by:

$$\frac{\partial V_m}{\partial Q_k} \approx \frac{1}{V}\sum_{i=1}^{\min(m,k)} X_i = \frac{1}{V}X^{\min(m,k)} \tag{5}$$

Here $V_m$ denotes the voltage magnitude at node $m$, $Q_k$ is the reactive power produced by the DG unit at node $k$, $X_i$ is the line reactance between the ($i$-1)-th and $i$-th node, and $V$ is the nominal network voltage.

Assuming the voltage regulation of node $m$ by the DG unit located at node $k$, the required reactive power variation depends on the relative position of node $k$ with respect to the regulated node $m$. Therefore, three cases are considered: In the first case, $k < m$, thus the voltage is regulated by a DG unit

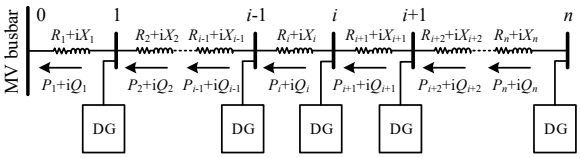


Fig. 2. Schematic diagram of a unidirectional generation feeder.

closer to the MV busbar. In the second case, $k = m$, while in the third one $k > m$, i.e., the DG unit is located further than the regulated node. The reactive power variations in the first and third cases, in relation to the second case are given in (6) and (7), respectively:

$$\frac{\Delta Q_{k<m}}{\Delta Q_{k=m}} = \frac{X^m}{X^k} > 1 \tag{6}$$

$$\frac{\Delta Q_{k>m}}{\Delta Q_{k=m}} = \frac{X^m}{X^m} = 1 \tag{7}$$

From (6), (7) it can be concluded that the required reactive power is minimized when the voltage is regulated by the DG unit located at the regulated node, or further than it with respect to the MV busbar. The corresponding feeder losses can be approximated by [16]:

$$P_{loss,k} \approx \frac{1}{V^2}\left[\sum_{i=1}^{n} R_i\left(\sum_{j=i}^{n} P_j\right)^2 + \sum_{i=1}^{k} R_i\left(\sum_{j=i}^{n} Q_j + \Delta Q_k\right)^2 + \sum_{i=k+1}^{n} R_i\left(\sum_{j=i}^{n} Q_j\right)^2\right] \tag{8}$$

$\Delta Q_k$ is the reactive power variation of the DG unit located at node $k$ and $R_i$ is the line resistance between the ($i$-1)-th and $i$-th node. Therefore, by substituting (6) and (7) in (8):

$$\frac{P_{loss,k\neq m}}{P_{loss,k=m}} > 1 \tag{9}$$

According to (9), the active power losses are minimized when the DG unit used for voltage regulation is located at the regulated node. This constitutes an important outcome on which the proposed control scheme is based. Furthermore, in this case, the reactive power variation is also minimized, as derived from (6) and (7). The condition in (9) applies under the assumption of constant $R/X$ ratio along the feeder, which is the normal case for a typical MV feeder.

### B. Application to the Generation Feeder

In case an overvoltage occurs at the generation feeder depicted in Fig. 2, the maximum voltage, and thus the regulated node, appears at the end of the feeder. Consequently, the DG unit at the last node will absorb reactive power to compensate the voltage rise and simultaneously attain minimum increase in the network losses.

The voltage rise in a single branch between two successive nodes is calculated according to,

$$V_{i-1}\cos\theta - V_i = -\frac{P_i R_i + Q_i X_i}{V_i} \tag{10}$$

$$\sin\theta = \frac{Q_i R_i - P_i X_i}{V_{i-1} V_i} \tag{11}$$

where, $V_{i\text{-}1}$ and $V_i$ are the voltage magnitudes, $\theta$ denotes the voltage angle difference, and $P_i$, $Q_i$ is the active and reactive power flowing through the branch, respectively. If the DG units are located at nodes close to the end of the feeder, the loading of the corresponding branches is relatively small, resulting in a negligible voltage angle difference between successive nodes. In such a case, the voltage rise between these nodes is zeroed when the reactive power flowing through the branch is equal to

$$Q_i = -\frac{R_i}{X_i} P_i \,. \tag{12}$$

When the DG unit at the last node operates according to (12), the voltages of the last two nodes are equal. At this point, the node before the last one becomes the regulated node and the corresponding DG unit undertakes the voltage regulation control. This process continues with the rest of DG units along the feeder until the overall voltage regulation is accomplished. Therefore, following this control scheme, the DG penetration is only restricted by the thermal limit of the line, since the voltage is fully controlled by the DG units.

Under maximum generation conditions, the DG units responsible for voltage regulation should be able to absorb reactive power equal to (12), which corresponds to a minimum power factor operation. This minimum power factor is proportional to the *R*/*X* ratio of the branch between the regulated node and the previous one. Thus, the resulting oversizing factor of the DG unit located at the *i*-th node is calculated according to:

$$D_i = \sqrt{1 + \left(\frac{R_i}{X_i}\right)^2} \tag{13}$$

The oversizing of the DG units according to (13) is a necessary condition for the proposed reactive power control scheme. It is only applied to the DG units of the last nodes, where overvoltages are more likely to occur. The remaining units operate with unity power factor and thus the oversizing is not necessary. The number of the oversized DG units, starting from the end node, is determined by a simple power flow analysis. As the DG units operate in under excited mode only, the limiting factor concerning their reactive power capability is the DG unit current, i.e. the apparent power, as analyzed in the Appendix. Therefore, the reactive power capability of every DG unit can be defined as follows:

$$Q_{\max,i} = \sqrt{\left(D_i P_{\max,i}\right)^2 - \left(P_i\right)^2} \tag{14}$$

where $Q_{\max,i}$ is the maximum reactive power the DG unit can provide in each time instant, $P_{\max,i}$, is the maximum active power of the DG unit, and $P_i$ is the active power injection at the specific time instant.

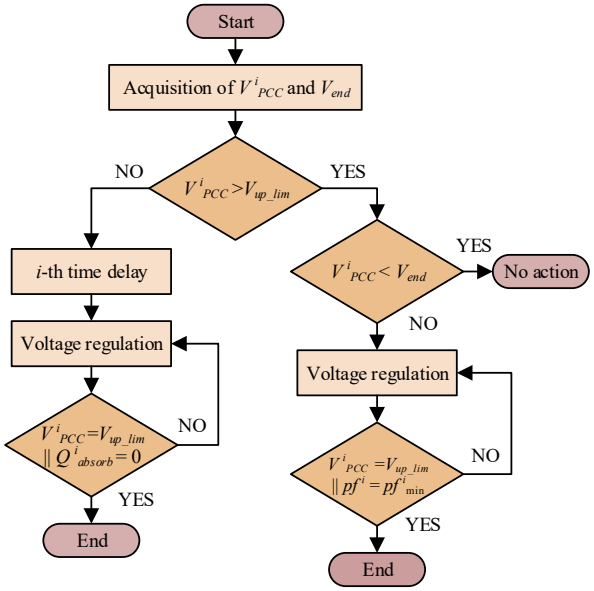


Fig. 3. Voltage regulation flowchart of the *i*-th DG unit.

Furthermore, the *R*/*X* ratio of typical overhead MV lines is normally less than 1, which corresponds to minimum power factor of approximately 0.7 lagging and an oversizing factor of less than 1.41. In the case of inverter-interfaced DG units, the efficiency of the inverter remains high, whereas the cost for the additional oversizing is low [24].

### C. *Actual Implementation*

A nearly decentralized voltage control scheme is proposed based on the previous analysis. The reactive power allocation among DG units is used to minimize the network losses and the total reactive power consumption. The developed algorithm, which is only applied to the oversized DG units, is presented in Fig. 3 by means of a flowchart.

More specifically, each DG unit measures the voltage magnitude at its PCC ($V_{PCC}$) and also receives information about the voltage at the last node ($V_{end}$). The latter can be transferred along the feeder using power line communication to avoid further communication infrastructure. When $V_{PCC}$ exceeds the upper voltage limit ($V_{up\_lim}$), the DG unit controller checks whether $V_{end}$ is larger than $V_{PCC}$. If so, no action is taken since the DG units located closer to the last node still absorb reactive power without having reached the minimum allowable power factor. Otherwise, the voltage regulation process is activated and the DG unit starts absorbing reactive power until the overvoltage is mitigated or the minimum power factor is reached. This process is implemented by employing proportional-integral (PI) controllers to eliminate the error between $V_{PCC}$ and $V_{up\_lim}$. After the voltage regulation is accomplished, the DG units that have reached the minimum power factor continue to operate in constant power factor mode.

The second part of the algorithm refers to the reverse process of reducing the reactive power absorption. Thus, in case the $V_{PCC}$ falls below the $V_{up\_lim}$, the DG unit reduces the

reactive power absorption till the $V_{PCC}$ reaches $V_{up\_lim}$ or the power factor becomes unity. However, a time delay is introduced in each DG unit to ensure the sequential activation of the voltage regulation process among them. Therefore, the oversized DG unit closer to the HV/MV transformer will instantly react in these voltage variations, whereas the DG unit at the end of the feeder will be the last to react. In this way, the simultaneous interactions among the PI controllers of the DG units are avoided [25], whereas the reactive power absorption and the active power losses are minimized. The time delay between two DG units located at successive nodes depends on their corresponding responses. In case of inverter-interfaced DG units, which have generally small response times, this value can be of order of few hundreds of milliseconds.

It is worth mentioning that the proposed voltage control scheme can be generalized for a tree-like generation feeder, provided that each DG unit receives voltage information from all ending nodes located downstream of it. The overvoltage mitigation process is activated when $V_{PCC}$ is equal to the voltage of every ending node, which means that all the downstream DG units have reached their minimum power factor. The reverse process of reducing the reactive power absorption is implemented by applying time delays to the DG units as previously mentioned.

## IV. Coordination with OLTC

The proposed reactive power control ensures the voltage regulation along the generation feeder, independently of the OLTC operation. The main objective of the proposed OLTC control is to reduce the network losses due to the reactive power control, while maintaining the voltages within permissible limits. The voltages along the mixed feeder are between the corresponding of the generation and the consumption feeders, since loads are partially fed by the local DG units. Therefore the limits for the voltages at the consumption feeders set the restrictions on the OLTC control.

DSOs in Europe must comply with the Standard EN 50160 concerning voltage operating limits, defined as ±10 % of the nominal voltage [26]. In case of consumption and mixed MV feeders, where LV distribution networks are connected, the limits at the MV level are generally reduced to ±5 % to ensure sufficient voltage regulation margin at the LV level. Therefore, the maximum allowable voltage at the MV busbar is considered equal to 1.05 pu.

The concept of the proposed OLTC operation is described as follows. During high generation periods, the DG units absorb reactive power to regulate the voltage which results in increased network losses. The OLTC aims to alleviate this reactive power absorption and thus to reduce the losses of the generation feeders by reducing the voltage at the MV busbar. However, this action is performed only when the voltage limits at the consumption feeders are not violated, since voltage regulation at these feeders is considered as the main priority of the OLTC. Therefore, the OLTC operation is formulated mathematically according to

$$Tap_{i+1} = \begin{cases} Tap_i + 1, & \text{if } V_{cons}^{i+1} > V_{\min} \text{ and } V_{gener}^{i} > V_{thres} \\ Tap_i - 1, & \text{if } V_{MV}^{i+1} < 1.05 \text{ and} \\ & \quad V_{cons}^{i} < V_{\min} \text{ or } V_{gener}^{i+1} < V_{thres} \\ Tap_i, & \text{otherwise} \end{cases} \quad (15)$$

$$V_{cons}^{i+1} = V_{cons}^{i} - \Delta V,\ V_{gener}^{i+1} = V_{gener}^{i} + \Delta V,\ V_{MV}^{i+1} = V_{MV}^{i} + \Delta V$$

where $Tap_i$ denotes the position of the tap changer at time $i$, $V_{min}$ is the minimum permissible voltage equal to 0.95 pu, and $V^i_{cons}$, $V^i_{gener}$ are the last node voltages of the consumption and generation feeders respectively at time $i$. $\Delta V$ is the magnitude of the voltage change per tap step, which occurs in each node. This value equals to the tap-changer step plus a configurable small dead band in order to consider the small impact of the changing loading conditions. In the cases examined in this paper, the dead band was set equal to 0.001 pu. In practice, the dead band can be estimated by the DSO, taking into account the actual load variations mainly in the consumption feeder. $V_{MV}$ is the voltage magnitude at the MV busbar, whereas $V_{thres}$ is the voltage threshold indicating the approach of the overvoltage limit. In this paper, the threshold is considered equal to 1.09 pu. Prior to any tap change, one minute time delay is applied in order to reduce the sensitivity of the OLTC control.

## V. Simulation Results

The proposed voltage regulation method is demonstrated in the MV network configuration shown in Fig. 1, where the mixed generation-consumption feeder is neglected. The remaining two feeders are identical, consisting of 10 nodes each, while the corresponding distances are presented in Table I. The impedance and the thermal limit of the line are 0.404 + i0.386 Ω/km and 296 A, respectively. In this network, only one type of DG is considered, i.e. PV units. The rated active power of PV units and loads, which are numbered according to their connection node, is shown in Table II. Simple power-flow calculations reveal that only the inverters of the PV units located at the last three nodes of the feeder need to be oversized according to (13), to achieve effective voltage regulation, during peak power injection. The power

TABLE I
Line Lengths at Each Feeder

| **Line** | **MV – 1** | **1 - 2** | **2 - 3** | **3 – 4** | **4 - 5** |
|---|---|---|---|---|---|
| **Length (km)** | 2 | 3 | 2 | 2 | 1 |
| **Line** | **5 – 6** | **6 - 7** | **7 - 8** | **8 - 9** | **9 - 10** |
| **Length (km)** | 3 | 2 | 3 | 4 | 3 |

TABLE II
Rated Active Power Generation and Consumption

| **PV unit** | **PV 1** | **PV 2** | **PV 3** | **PV 4** | **PV 5** |
|---|---|---|---|---|---|
| **MW** | 0.8 | 0.5 | 1.5 | 0.5 | 0.5 |
| **PV unit** | **PV 6** | **PV 7** | **PV 8** | **PV 9** | **PV 10** |
| **MW** | 1 | 1.5 | 1.5 | 2 | 0.8 |
| **Load** | **Load 1** | **Load 2** | **Load 3** | **Load 4** | **Load 5** |
| **MW** | 0.75 | 0.25 | 0.8 | 1 | 0.5 |
| **Load** | **Load 6** | **Load 7** | **Load 8** | **Load 9** | **Load 10** |
| **MW** | 0.8 | 0.5 | 0.7 | 0.25 | 0.5 |

factor of all loads is considered constant and equal to 0.95 inductive. The transformer connection is a 150 kV/20 kV, Dy5 with a rated power of 250 MVA, short-circuit voltage of 12 %, while the full-load losses are 0.3 %. The transformer tap range is ±8 with a voltage variation of 1.67 % per tap.

Initially, the results obtained from a time-domain simulation are presented to highlight the effectiveness and the fast response of the proposed control. In the second subsection, the improved performance of the control is demonstrated by comparing it with well-known control schemes via a time-series, quasi-static power flow simulation.

### *A. Time-domain simulation*

The generation feeder is modelled at the PSIM software where the reactive power control is applied to the last three PV units, which are equipped with oversized inverters. A direct-quadrature rotating frame control method is employed in each grid-interfaced inverter. The voltage at the beginning of the feeder is considered constant and equal to 1.05 pu, whereas the time delay for the activation of voltage regulation between two successive PV units is 0.25 s. The communication delay is considered equal to 0.03 s. These values, which are fully configurable, have been chosen to reduce the overall simulation time. The PV units inject their rated active power except those with variable output that are depicted in Fig. 4. This can occur in extended MV networks due to varying sky conditions over PV units in distance. The reactive power consumption of the last three PV units is illustrated in Fig. 5, whereas the corresponding PCC voltages are presented in Fig. 6.

Prior to 0.5 s, the PCC voltages are below the maximum allowable voltage defined at 1.1 pu and thus the voltage regulation process remains deactivated. At 0.5 s, a step increase of the injected active power of some PV units occurs as shown in Fig. 4. As a consequence, the upper voltage threshold is violated and overvoltages occur along the feeder. According to Fig. 6, the maximum voltage appears at PV10, which starts absorbing reactive power to regulate the voltage at the PCC. The voltage regulation processes of PV8 and PV9 remain deactivated since the corresponding voltages are lower than the voltage of PV10.

At 0.59 s, the voltage of PV10 becomes equal to the corresponding of PV9. In fact, due to the nonzero voltage angle $\theta$ in (10), the voltage of PV10 will be slightly less than the corresponding of PV9, which, however, does not affect the voltage regulation procedure. PV9 interprets this as a signal that minimum power factor operation is reached by the PV10, also verified in Fig. 5. Since the PCC voltage of PV9 remains above 1.1 pu, the voltage regulation process of this unit is activated. At 0.72 s, the voltages of PV9 and PV10 become both equal to the corresponding of PV8 and since the overvoltage at PV8 persists, its inverter starts absorbing reactive power till the voltage is finally regulated at the time instant of 1 s. In this way, minimum reactive power consumption and consequently minimum network power losses are achieved.

The second part of the proposed algorithm is implemented

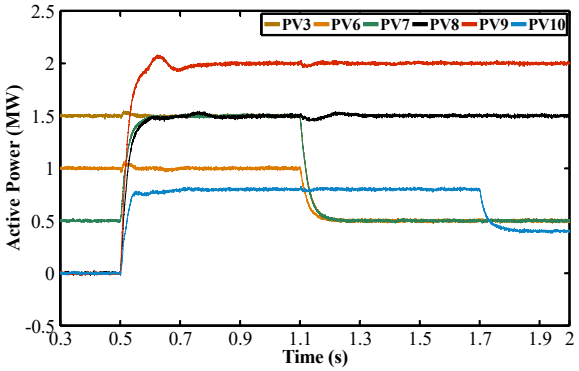


Fig. 4. Injected active power of PV units.

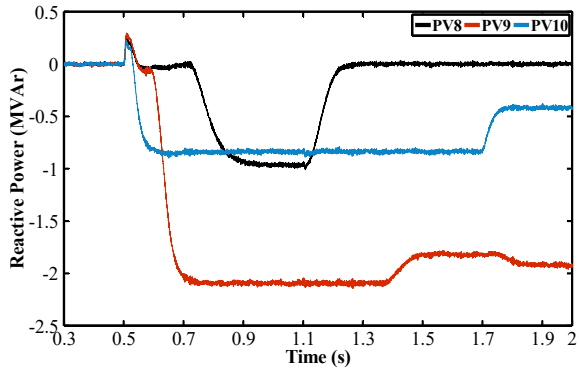


Fig. 5. Absorbed reactive power of PV units.

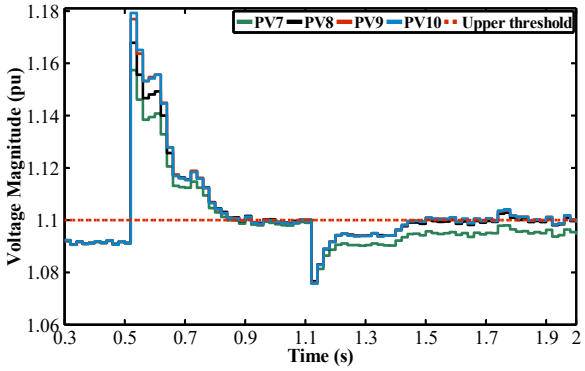


Fig. 6. Voltage at the PCC of PV units.

by reducing simultaneously the active power injections of PV3, PV6 and PV7 at the time 1.1 s, as shown in Fig. 4. The last three PV units sense this generation reduction by the corresponding decrease of their PCC voltages. However, they do not react immediately due to the different time delays introduced in each of them. The PV8 is the first to react, decreasing the reactive power consumption in order to recover the PCC voltage back to the upper threshold. Due to the fast response of the inverter, the reactive power of PV8 is zeroed at 1.25 s. However, the voltage still remains below the upper threshold. Then, after a time delay of 0.25 s, PV9 starts reducing its reactive power consumption till voltage regulation is accomplished at 1.5 s.

At 1.7 s, the active power of PV10 is assumed to decrease and since it operates with the minimum power factor, the reactive power will instantly change as shown in Fig. 5. As a

consequence, the reactive power of PV9, where the voltage regulation process is already activated from the previous stage, will also change in order to maintain the voltage equal to the 1.1 pu, ensuring minimum losses and reactive power consumption.

### *B. Quasi-static simulation*

In this section, time-series simulations are performed to compare the proposed voltage regulation algorithm with other widely-used decentralized control schemes and a centralized optimal-power-flow-based method. More specifically, the $Q(P)$ and $Q(V)$ characteristics are applied to the PV units of the generation feeder following the coordination procedure proposed in [17] and [18], respectively. For this purpose, the simulation tool developed in [27] is used in order to efficiently conduct the simulations. Additionally, the optimal power flow (OPF) method aims at minimizing the network losses by properly allocating the reactive power consumption among PV units and considering the maximum allowable voltage as the only operational constrain. This non-linear problem is solved using the interior point method that performs well due to the relative small size of the examined network. However, in order to ensure the global optimality of the OPF method, a Monte Carlo approach is employed to generate random values for the initial points of this method forming the optimal power flow with Monte Carlo (OPF-MC) method. In this method, 1000 initial points are randomly created for the OPF in each time instant.

The application of the control schemes described previously guaranties that the overvoltage limit is not violated along the feeder. Therefore, the power injection can be increased up to the line thermal limit, which is now the limiting constraint. To evaluate the performance of the different controls, the maximum penetration range (MPR) is introduced. For each case, MPR is limited by the maximum line thermal current and is calculated following the distribution of the active power generation per node, as shown in Table II. The different control schemes result in the MPRs of Table III. It can be seen that the maximum MPR appears when the OPF method is applied which coincides with the OPF-MC. Although the resulting MPR by the proposed method is less than the corresponding of the OPF, it still remains much higher compared to MPR of the decentralized control schemes. Therefore, the minimum MPR caused by the $Q(P)$ characteristic is chosen as a comparable basis for the time-series simulations.

TABLE III
MAXIMUM PENETRATION AT THE GENERATION FEEDER

| | OPF-MC | OPF | Q(P) | Q(V) | Proposed |
|---|---|---|---|---|---|
| **Total Installed Capacity (MW)** | 11.55 | 11.55 | 9.54 | 9.83 | 10.60 |
| **Diff (%)** | | 0 | -17.43 | -14.95 | -8.26 |

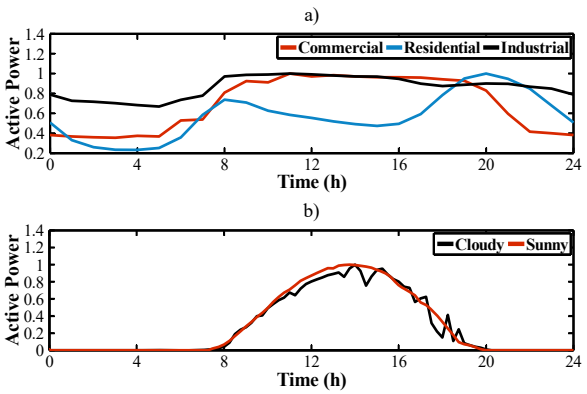


Fig. 7. Normalized active power profiles. (a) Load profiles and (b) generation profiles.

The simulation time frame is one day. Normalized typical load profiles for different consumer categories, as well as generation profiles as shown in Fig. 7 are randomly distributed to the consumption and generation feeders, respectively. These profiles are multiplied with the rated power of each load or PV unit to obtain the daily load or generation profile at each bus. Initially, a conventional operation of the OLTC is considered, i.e. the voltage at the MV busbar is kept close to 1.05 pu which, in the examined network, corresponds to a tap position equal to -3, remaining constant for all the simulation period. The voltage profile of PV10 located at the last node of the generation feeder is depicted in Fig. 8, whereas the total reactive power consumption of the PV units is shown in Fig. 9.

Considering the $Q(P)$ characteristic, the main drawback is that this control does not take into account the network operational condition, since the absorbed reactive power in each PV unit depends only on the corresponding active power injection. Therefore, in cases of divergences in PV

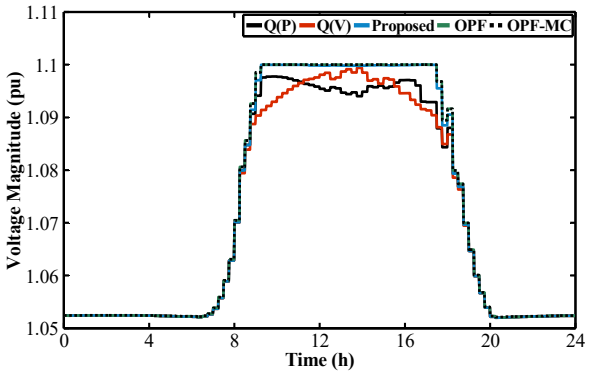


Fig. 8. Voltage profile of PV10.

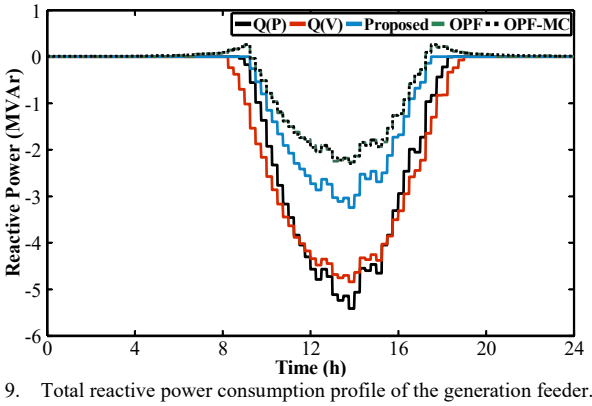


Fig. 9. Total reactive power consumption profile of the generation feeder.

generated power, due to local clouds, which is very a common situation in MV networks due to the large covering area, the consumption of the reactive power is unnecessary high resulting in voltages far below the upper threshold, as verified in Fig. 8, and thus in increased active power losses.

This situation is improved by the introduction of the $Q(V)$ control where the reactive power consumption is activated after the PCC voltage exceeds the droop threshold, which is lower than the maximum allowable voltage. Therefore, the PV units start absorbing reactive power from a lower overvoltage and this results in increased active power losses and a bell-shaped voltage profile as shown in Fig. 8. On the other hand, the proposed voltage control aims at maintaining voltages close to the upper voltage limit to ensure minimum reactive power consumption and losses, as illustrated in Fig. 9.

The OPF results in minimum reactive power consumption compared to the other methods, whereas the voltage profile is similar to the corresponding of the proposed method. This is also verified with the OPF-MC method since the corresponding curves overlap. The total daily energy losses are presented in the first column of Table IV, where it is observed that the proposed method achieves almost up to 7 % reduction in the total energy losses compared to the decentralized control methods, slightly higher than the OPF and OPF-MC methods. This benefit of the OPF cannot compensate the extensive communication infrastructure needed for implementing this method, compared to the corresponding low requirements of the proposed control.

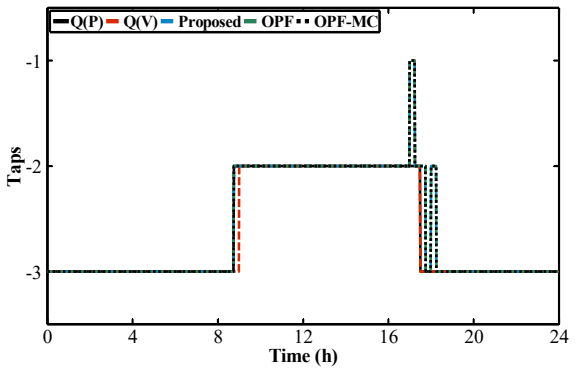


Fig. 10. Tap variation profile.

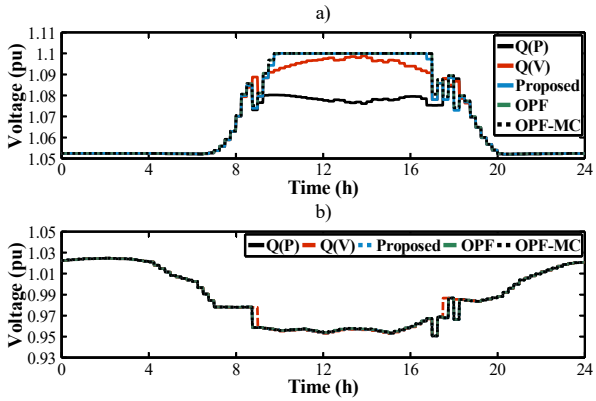


Fig. 11. Voltage profile. (a) PV10 and (b) Load10.

TABLE IV
ENERGY LOSSES (MWH)

| | Conventional OLTC | Proposed OLTC | Difference (%) |
|---|---|---|---|
| **Q(P)** | 8.42 | 8.66 | 2.85 |
| **Q(V)** | 8.38 | 7.89 | -5.90 |
| **Proposed** | 7.98 | 7.73 | -3.13 |
| **OPF** | 7.95 | 7.70 | -3.14 |
| **OPF-MC** | 7.95 | 7.70 | -3.14 |

Moreover, all the PV units of the generation feeder operate with oversized inverters in the OPF method, whereas in the proposed control only part of the inverters, in this case the last three PV units, need to be oversized.

Finally, OLTC control is introduced in order to further reduce the active power losses. In Fig. 10, the tap variation of the OLTC is depicted and the voltage profiles along the feeders are shown in Fig. 11. The corresponding daily energy losses are presented in the second column of Table IV. The use of the OLTC control reduces the reactive power consumption of the PV units, and thus the energy losses, since it reduces the voltage magnitude at the MV busbar, while maintaining the voltages of the consumption feeder within operating limits. The active power losses are only increased in the case of the $Q(P)$ implementation, since this control ignores the network operational condition. Consequently, the optimal network operation by means of minimizing reactive power consumption and losses is ensured by the combined operation of the OLTC control with the proposed voltage control.

## VI. DISCUSSION AND CONCLUSIONS

In this paper, a nearly decentralized voltage control method is proposed, coordinating in an optimal way the reactive power allocation among the DG units of a feeder to minimize network losses in a MV distribution network. This is achieved by operating the feeder close to the allowable upper overvoltage limit. A method for determining the number and the required oversizing of the DG units that will participate in the voltage regulation is presented. The proposed control method needs only the reading of the RMS voltage at the end-node of the feeder, thus minimizing communication infrastructure requirements. The proposed control method is enhanced using a modified control of the OLTC operation to further reduce the network losses. Simulation results justify the robustness and the improved performance of the proposed method over conventional decentralized control schemes.

The nodes with overvoltages are determined by the DG penetration level. Therefore, in cases of low penetration levels, the expected overvoltages are smaller and consequently the effectiveness of the proposed reactive power control is ensured. Moreover, the absorbed reactive power of each DG unit participating in the voltage regulation process aims to compensate the voltage rise caused by the corresponding active power injection. So, the disconnection of such a DG unit, e.g. in case of fault, will not affect the voltage at the PCC and thus the performance of the proposed reactive power control.

Furthermore, the number of the DG units participating in

the reactive control scheme is determined by a simple power flow. In cases where DG units with low rated power are connected at the nodes close to the feeder end, the control scheme will include further DG units, more remotely located, to mitigate overvoltage efficiently.

The proposed reactive power control is employed at the generation feeders, where reverse power flow occurs. In case DSOs allow a greater DG penetration at the mixed generation-consumption feeders, a similar control scheme should be applied. However, the bidirectional power flow, which is a typical characteristic of these feeders, may lead to time-varying voltage profiles, e.g. increasing, bell-shaped, decreasing, etc. Furthermore, the presence of loads affects the oversizing of the DG units, since the active and reactive power consumptions reduce the oversizing factor. However, the proposed methodology can be properly modified to take into account these issues and this constitutes part of future research work.

## APPENDIX

Following the procedure presented in [20], the reactive power capability of the DG unit shown in Fig. 12, is determined by two limiting factors, namely the maximum value of the internal voltage ($V_e$) and the current limit. According to the proposed voltage regulation method, the DG units participating in this process will operate in under excited mode, absorbing reactive power. In such a case, the maximum value of $V_e$, and thus the respective DC voltage in the case of inverter-interfaced DG units, is not a limiting factor, since it will be lower than $V_{PCC}$. This can be also verified by the active ($P$) and reactive power ($Q$) injections, given by,

$$P = \frac{V_e V_{PCC}}{X_c} \sin\delta \tag{A.1}$$

$$Q = \frac{V_e V_{PCC}}{X_c} \cos\delta - \frac{V_{PCC}^2}{X_c} \tag{A.2}$$

where $\delta$ is the load angle and $X_c$ is the equivalent output reactance. In the case of inverter-interfaced DG units, $X_c$ is the aggregated reactance of the output filter and of the MV/LV transformer, when present, while in the case of synchronous generators, it denotes the synchronous reactance.

However, a relatively low $V_e$ may result to stability issues, which limit the absorbed reactive power. Thus, the reactive power capability of the DG unit is now determined by two limiting factors, i.e. the current and the stability limit. The former, results in the reactive power capability given by (14), whereas the latter introduces a maximum operational limit for the load angle. When the voltage regulation process is activated, the PCC voltage is equal to 1.1 pu. Therefore, under maximum generation conditions, the maximum permissible $X_c$ can be calculated with respect to the oversizing factor and the load angle according to:

$$X_c^{\max} = \frac{1.21}{\sqrt{D^2 - 1} + \cot\delta_{\max}} \tag{A.3}$$

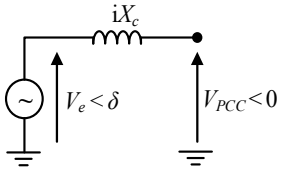


Fig. 12. Simplified equivalent circuit of a DG unit.

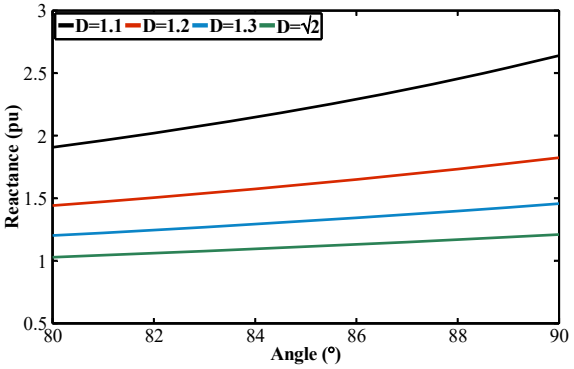


Fig. 13. Upper limit of the output reactance.

Eq. (A.3) is derived from (A.2), (A.3), and (14), assuming maximum allowable load angle $\delta_{\max}$. It is noted that, with inverter-interfaced DG units, $\delta_{\max}$ equals to 90º, since there are no masses, thus no dynamic stability margins.

The maximum permissible output reactance for the different values of $D$ is shown in Fig. 13, where it is evident that in all cases $X_c$ should be larger than 1 pu for the stability limit to become binding. In the case of inverter-interfaced DG units, a common value of the $X_c$ is 0.3-0.4 pu [20], which is much lower than the above shown limits. On the other hand, synchronous generators can be properly designed so as to operate with an appropriate power factor, when injecting their peak power, avoiding this problem.

Therefore, the reactive power capability of the DG units is only determined by the corresponding current limit, i.e. the maximum apparent power and the active power loading as given in (14).

## REFERENCES


[1] *On the Promotion of the Use of Energy from Renewable Sources and Amending and Subsequently Repealing Directives 2001/77/EC and 2003/30/EC*, Directive 2009/28/EC, European Parliament and Council, Brussels, Belgium, 2009, pp. 16-62.

[2] R. A. R. Walling, R. Saint, R. C. Dugan, J. Burke, and L. A. Kojovic, "Summary of distributed resources impact on power delivery system," *IEEE Trans. Power Del.*, vol. 23, no. 3, pp. 1636–1644, Jul. 2008.

[3] C. L. Masters, "Voltage rise: The big issue when connecting embedded generation to long 11 kV overhead lines," *Power Eng. J.*, vol. 16, no. 1, pp. 5-12, Feb. 2002.

[4] M. E. Elkhatib, R. El-Shatshat, M. M. A. Salama, "Novel coordinated voltage control for smart distribution networks with DG," *IEEE Trans. Smart Grid*, vol. 2, no. 4, pp. 598–605, Dec. 2011.

[5] M. E. Baran and I. M. El-Markabi, "A multiagent-based dispatching scheme for distributed generators for voltage support on distribution feeders," *IEEE Trans. Power Syst.*, vol. 22, no. 1, pp. 52–59, Feb. 2007.

[6] H. E. Farag, E. F. El-Saadany, and R. Seethapathy, "A two ways communication-based distributed control for voltage regulation in smart distribution feeders," *IEEE Trans. Smart Grid*, vol. 3, no. 1, pp. 271–281, Mar. 2012.

[7] H. E. Z. Farag and E. F. El-Saadany, "A novel cooperative protocol for distributed voltage control in active distribution systems," *IEEE Trans. Power Syst.*, vol. 28, no. 2, pp. 1645–1656, May 2013.
[8] V. Calderaro, V. Galdi, F. Lamberti, and A. Piccolo, "A smart strategy for voltage control ancillary service in distribution networks," *IEEE Trans. Power Syst.*, vol. 30, no. 1, pp. 494–502, Jan. 2015.
[9] P. N. Vovos, A. E. Kiprakis, A. R. Wallace, and G. P. Harrison, "Centralized and distributed voltage control: Impact on distributed generation penetration," *IEEE Trans. Power Syst.*, vol. 22, no. 1, pp. 476–483, Feb. 2007.
[10] L. F. Ochoa, A. Keane, and G. P. Harrison, "Minimizing the reactive support for distributed generation: Enhanced passive operation and smart distribution networks," *IEEE Trans. Power Syst.*, vol. 26, no. 4, pp. 2134–2142, Nov. 2011.
[11] A. Vaccaro, G. Velotto, and A. F. Zobaa, "A decentralized and cooperative architecture for optimal voltage regulation in smart grids," *IEEE Trans. Ind. Electron.*, vol. 58, no. 10, pp. 4593–4602, Oct. 2011.
[12] B. A. Robbins, C. N. Hadjicostis, and A. D. Dominguez-Garcia, "A two-stage distributed architecture for voltage control in power distribution systems," *IEEE Trans. Power Syst.*, vol. 28, no. 2, pp. 1470–1482, May 2013.
[13] P. M. S. Carvalho, P. F. Correia, and L. A. F. M. Ferreira, "Distributed reactive power generation control for voltage rise mitigation in distribution networks," *IEEE Trans. Power Syst.*, vol. 23, no. 2, pp. 766–772, May 2008.
[14] K. Turitsyn, P. Sulc, S. Backhaus, and M. Chertkov, "Local control of reactive power by distributed photovoltaic generators," in *Proc. First IEEE Int. Conf. Smart Grid Communications*, Gaithersburg, MD, USA, 2010, pp. 79-84.
[15] K. Turitsyn, P. Sulc, S. Backhaus, and M. Chertkov, "Options for control of reactive power by distributed photovoltaic generators," *Proc. IEEE*, vol. 99, no. 6, pp. 1063–1073, June 2011.
[16] H.-G. Yeh, D. F. Gayme, and S. H. Low, "Adaptive VAR control for distribution circuits with photovoltaic generators," *IEEE Trans. Power Syst.*, vol. 27, no. 3, pp. 1656–1663, Aug. 2012.
[17] A. Samadi, R. Eriksson, L. Söder, B. G. Rawn, and J. C. Boemer, "Coordinated active power-dependent voltage regulation in distribution grids with PV systems," *IEEE Trans. Power Del.*, vol. 29, no. 3, pp. 1454–1464, June 2014.
[18] A. Samadi, E. Shayesteh, R. Eriksson, B. Rawn, and L. Söder, "Multi-objective coordinated droop-based voltage regulation in distribution grids with PV systems," *Renew. Energy*, vol. 71, pp. 315–323, Nov. 2014.
[19] V. Calderaro, G. Conio, V. Galdi, G. Massa, and A. Piccolo, "Active management of renewable energy sources for maximizing power production," *Int. J. Elect. Power Energy Syst.*, vol. 57, pp. 64–72, May 2014.
[20] V. Calderaro, G. Conio, V. Galdi, G. Massa, and A. Piccolo, "Optimal decentralized voltage control for distribution systems with inverter-based distributed generators," *IEEE Trans. Power Syst.*, vol. 29, no. 1, pp. 230–241, Jan. 2014.
[21] K. Tanaka, M. Oshiro, S. Toma, A. Yona, T. Senjyu, T. Funabashi, and C. H. Kim, "Decentralized control of voltage in distribution systems by distributed generators," *IET Gener. Transm. Distrib.*, vol. 4, no. 11, pp. 1251–1260, Nov. 2010.
[22] T. Stetz, F. Marten, and M. Braun, "Improved low voltage grid-integration of photovoltaic systems in Germany," *IEEE Trans. Sustain. Energy*, vol. 4, no. 2, pp. 534–542, Apr. 2013.
[23] M. Brenna *et al.*, "Automatic distributed voltage control algorithm in smart grids applications," *IEEE Trans. Smart Grid*, vol. 4, no. 2, pp. 877–885, June 2013.
[24] C. Demoulias, "A new simple analytical method for calculating the optimum inverter size in grid-connected PV plants," *Elect. Power Syst. Res.*, vol. 80, no. 10, pp. 1197–1204, Oct. 2010.
[25] H. Li, F. Li, Y. Xu, D. T. Rizy, and S. Adhikari, "Autonomous and adaptive voltage control using multiple distributed energy resources," *IEEE Trans. Power Syst.*, vol. 28, no. 2, pp. 718–730, May 2013.
[26] *Voltage characteristics of electricity supplied by public distribution networks*, Standard EN 50160:2010.
[27] G. C. Kryonidis *et al.*, "A simulation tool for extended distribution grids with controlled distributed generation," in *Proc. 2015 IEEE Eindhoven PowerTech*, Eindhoven, Netherlands, pp. 1–6.

**Georgios C. Kryonidis** (S'12) received the Dipl. Eng. Degree from the School of Electrical and Computer Engineering at the Aristotle University of Thessaloniki, in 2013. Since 2013, he has been a Ph.D. candidate at the same university. His research interests are in the field of distributed generation and smart grids.

**Charis S. Demoulias** (M'96–SM'11) received the Diploma and Ph.D. degrees in electrical engineering from the Aristotle University of Thessaloniki, where he is currently Assistant Professor with the Electrical Machines Laboratory. His research interests include power electronics, harmonics, electric motion systems, and renewable energy sources.

**Grigoris K. Papagiannis** (S'79–M'88–SM'09) received his Dipl. Eng. Degree and the Ph.D. degree from the School of Electrical and Computer Engineering at the Aristotle University of Thessaloniki, where he is currently Professor and Director of the Power Systems Laboratory. His special interests are power systems modelling, computation of electromagnetic transients, distributed generation and power-line communications.